

ORIGINAL ARTICLE

Synergistic proapoptotic effects of the two tyrosine kinase inhibitors pazopanib and lapatinib on multiple carcinoma cell linesKA Olaussen^{1,2,3,4,7}, F Commo^{2,3,7}, M Tailler^{1,2,4}, L Lacroix^{2,3}, I Vitale^{1,2,4}, SQ Raza^{1,2,4}, C Richon⁵, P Dessen⁵, V Lazar⁵, J-C Soria^{2,3,4,6,8} and G Kroemer^{1,2,4,8}¹INSERM, U848, Villejuif, France; ²Institut Gustave Roussy, Villejuif, France; ³Laboratoire de Recherche Translationnelle, Institut Gustave Roussy, Villejuif, France; ⁴Université Paris-Sud XI, Paris, France; ⁵Unité de Génomique fonctionnelle et Bioinformatique, Institut Gustave Roussy, Villejuif, France and ⁶Department of Medicine, Institut Gustave Roussy, Villejuif, France

Pazopanib and lapatinib are two tyrosine kinase inhibitors that have been designed to inhibit the VEGF tyrosine kinase receptors 1, 2 and 3 (pazopanib), and the HER1 and HER2 receptors in a dual manner (lapatinib). Pazopanib has also been reported to mediate inhibitory effect on a selected panel of additional tyrosine kinases such as PDGFR and c-kit. Here, we report that pazopanib and lapatinib act synergistically to induce apoptosis of A549 non-small-cell lung cancer cells. Systematic assessment of the kinome revealed that both pazopanib and lapatinib inhibited dozens of different tyrosine kinases and that their combination could suppress the activity of some tyrosine kinases (such as c-Met) that were not or only partially affected by either of the two agents alone. We also found that pazopanib and lapatinib induced selective changes in the transcriptome of A549 cells, some of which were specific for the combination of both agents. Analysis of a panel of unrelated human carcinoma cell lines revealed a signature of 52 genes whose up- or downregulation reflected the combined action of pazopanib and lapatinib. Indeed, pazopanib and lapatinib exerted synergistic cytotoxic effects on several distinct non-small-cell lung cancer cells as well as on unrelated carcinomas. Altogether, these results support the contention that combinations of tyrosine kinase inhibitors should be evaluated for synergistic antitumor effects. Such combinations may lead to a ‘collapse’ of pro-survival signal transduction pathways that leads to apoptotic cell death. *Oncogene* (2009) 28, 4249–4260; doi:10.1038/onc.2009.277; published online 14 September 2009

Keywords: pazopanib; lapatinib; TKIs; apoptosis; kinome; transcriptome

Introduction

The unwarranted survival of cancer cells relies on the constitutive activation of growth factor receptors, often tyrosine kinase receptors, that may be overactivated due to their overexpression, activating mutations and/or the continuous presence of their ligands. The continuous phosphorylation of their substrates on tyrosine residues then can improve the flux of metabolites through the plasma membrane (Flier *et al.*, 1987), a process that is essential for anabolic reactions required for tumor cell growth (Edinger, 2007). In addition, receptor tyrosine kinases signal for growth (Hult *et al.*, 2002), inhibition of cell death (Barnes and Kumar, 2003) as well as increased motility and angiogenesis (Petit *et al.*, 1997), thereby contributing to the phenotypic characteristics of cancer. For this reason, specific or general tyrosine kinase inhibitors have been developed for anticancer therapy, and spectacular progress has been achieved in the treatment of selected malignancies relying on the constitutive signaling of Bcr-Abl (chronic myeloid leukemia) (Druker *et al.*, 2001), c-kit (gastrointestinal stromal tumor, GIST) (Sleijfer *et al.*, 2008), HER2 (breast cancer) (Cameron and Stein, 2008) and HER1 (non-small-cell lung cancer, colorectal cancer, squamous cell head and neck cancer and pancreatic cancer) (Ciardiello and Tortora, 2008), among others (Noble *et al.*, 2004). As a result, tyrosine kinase inhibitors are under close scrutiny for the targeted therapy of multiple distinct neoplasias.

Pazopanib (GW786034B) is a multitarget kinase inhibitor that blocks the VEGF tyrosine kinase receptors 1, 2 and 3 (VEGFR-1, -2 and -3), which have a key function in the regulation of normal and pathological angiogenesis (Harris *et al.*, 2008). In addition, but to a lesser extent, pazopanib also inhibits PDGFR and c-kit (Kumar *et al.*, 2007). In xenograft models, pazopanib inhibits the growth of a broad range of human tumors including colon, lung, breast, renal and prostate carcinomas, chondrosarcoma, leiomyosarcoma, melanoma, multiple myeloma and GIST (Kumar *et al.*, 2007). Pazopanib is currently evaluated in a phase III clinical trial for the therapy of metastatic renal cell carcinoma (Sonpavde *et al.*, 2008). Although VEGFR inhibitors are commonly thought to act through an effect on tumor endothelial cells, thus preventing

Correspondence: Dr G Kroemer, INSERM, U848, Institut Gustave Roussy, 39 rue Camille Desmoulins, F-94805, Villejuif, France. E-mail: kroemer@igr.fr.

⁷These authors contributed equally to this work.

⁸These authors share senior co-authorship.

Received 17 April 2009; revised 8 July 2009; accepted 8 August 2009; published online 14 September 2009

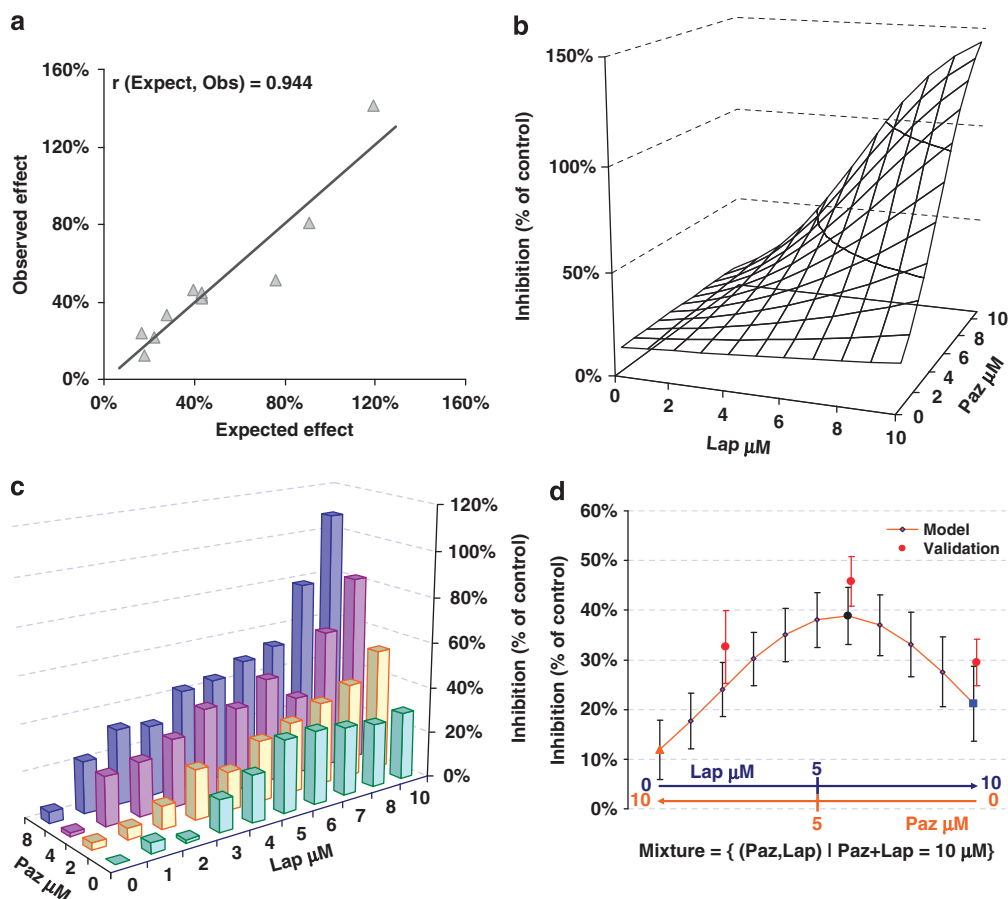


Figure 2 Synergistic action of pazopanib and lapatinib on A549 cells. (a) Correlation between observed and fitted responses by the linear model. A549 cells were treated for 72 h before the tetrazolium conversion assay. The drug concentrations were chosen following a rotatable matrix. The estimated IC_{50} values of pazopanib and lapatinib alone were > 20 and $10 \pm 2 \mu\text{M}$, respectively. A linear model of drug response was established using the following equation: $Y = \alpha + \gamma \cdot \text{Lap} + \delta \cdot \text{Paz} \cdot \text{Lap} + \epsilon_{(\text{resp})}$. An inhibition index from 0 to 200% was calculated as detailed in the Materials and methods section. If the score equals 0%, the effect is null (control condition). If the score is 100%, the number of cells equals the number at treatment start (T_0), which translates mainly a cytostatic effect. If the score is between 100 and 200%, the effect of drug treatment is cytotoxic. Dose response was transformed in $\text{Log}[E/(E_{\text{max}} - E)]$ to estimate the parameters, and reconverted into response in percent for graphic representation. (b) Estimated response surface fitted by the linear model, as calculated from the data summarized in a. (c) Validation by chessboard analysis of a new data set. A549 cells were treated with the indicated concentrations of pazopanip (Paz) and lapatinip (Lap) for 72 h before the colorimetric assessment of cell proliferation. (d) Graphical comparison between the model and observed values. The dotted line represents expected values from the model in b chosen as to always obtain a sum of total drug concentrations of $10 \mu\text{M}$ (isodose curve). The three red dots represent the corresponding observed values of the same mixture in the validation data set shown in c. A full colour version of this figure is available at the *Oncogene* journal online.

leading to the accumulation of cells with a subdiploid DNA content (Figure 3c). The combination of pazopanib and lapatinib also induced a reduction in clonogenic survival of A549 cells, in conditions in which pazopanib and lapatinib alone had minor or no effects (Figure 3d).

Taken together, these results indicate that pazopanib and lapatinib have synergistic cytotoxic effects on the survival of A549 cells that may be explained by the induction of apoptotic cell death.

Hyperadditive effects of pazopanib and lapatinib on the kinome and the transcriptome of A549 cells
Pazopanib and lapatinib have been developed as inhibitors of the VEGFR and HER1/HER2 receptors, respectively. The ensemble of kinases, the kinome, is

organized in a network of interacting cascades with multiple cross talks (Manning *et al.*, 2002; Johnson and Hunter, 2005). To study the effects of pazopanib and lapatinib on the kinome, we generated lysates from A549 cells that had been preincubated with pazopanib or lapatinib or both for 12 h—well before any kind of cytotoxic activity can be detected (data not shown)—and applied these lysates to peptides immobilized on glass slides. The activity of kinases contained in the lysate was then monitored by detecting phosphotyrosine residues using specific antibodies that were visualized by means of an immunochemical method (Figure 4a). Both lapatinib and pazopanib alone inhibited multiple kinases. The combination of both inhibitors yielded a hyperadditive effect on some kinase activities (Figure 4b; Supplementary Table S1), meaning that lapatinib and pazopanib in combination inhibited some

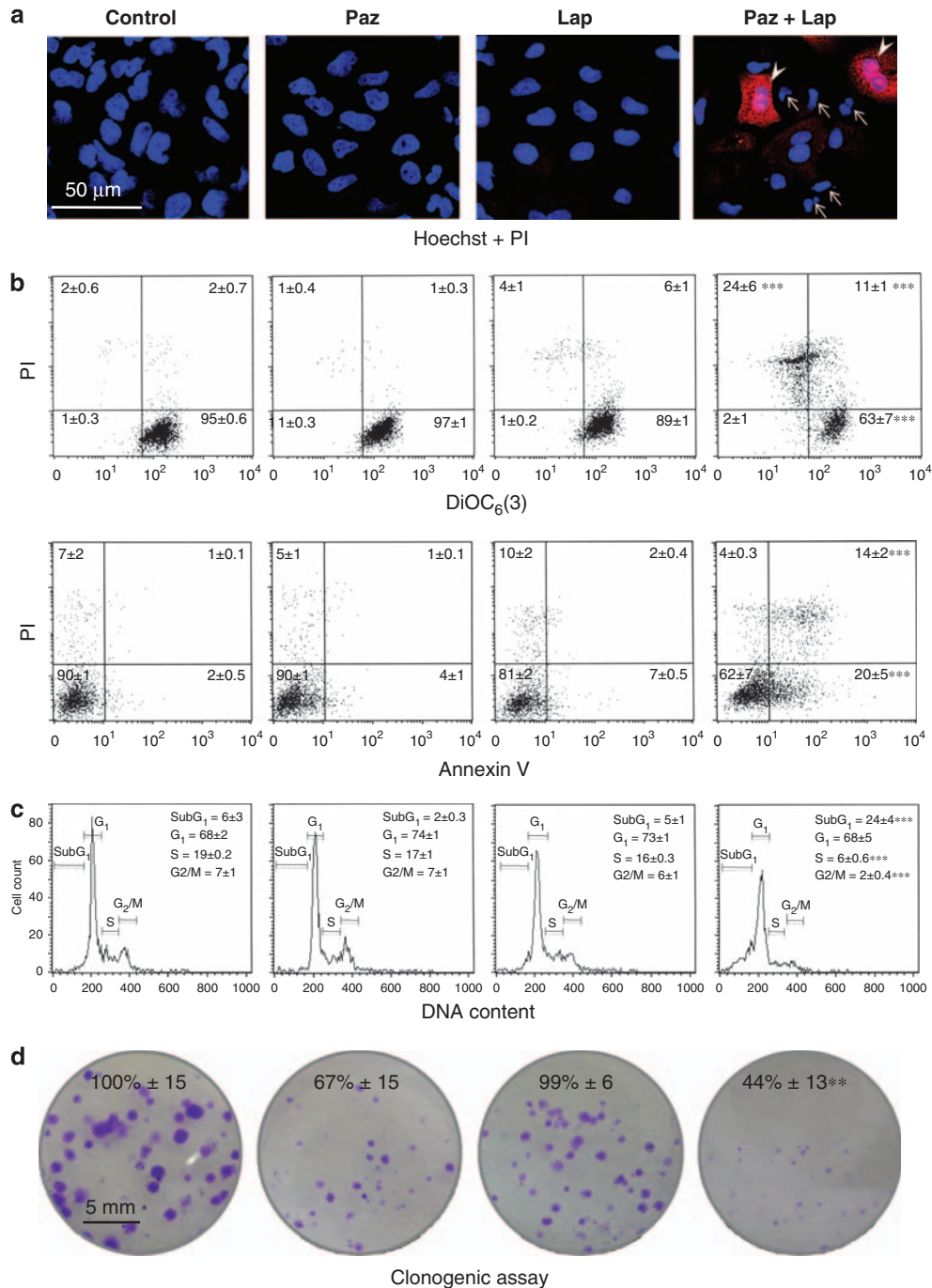


Figure 3 Proapoptotic effects of pazopanib/lapatinib on A549 cells. A549 cells were incubated in triplicate wells with 8 μM of pazopanib (Paz), or 10 μM of lapatinib (Lap) or both for 72 h, followed by assessment of cell-death-associated parameters. (a) Confocal fluorescence microscopy. A549 cells were stained with Hoechst 33342 (in blue) to visualize chromatin and with propidium iodide (PI, in red). Representative microphotographs chromatin condensation (arrows) or plasma membrane permeabilization (arrow heads) are shown. Note that a fraction of cells exhibit chromatin condensation and hence have undergone apoptosis. (b) Synergistic disruption of the mitochondrial transmembrane potential and induction of phosphatidylserine exposure by pazopanib plus lapatinib. A549 cells were treated as in a, stained with the potential sensitive dye DiOC₆(3) and PI or Annexin V-FITC plus PI, and then subjected to cytofluorimetric analysis. The mean percentages of cells in each quadrant of the dot plot are indicated \pm s.d. (triplicates). (c) DNA degradation induced by pazopanib plus lapatinib. Cells were subjected to Hoechst 33342 staining and to cytometric analysis of the DNA content. Mean percentages \pm s.d. of each cell population are provided. (d) Effect of pazopanib and lapatinib on the clonogenic potential of A549 cells. Cells were treated as elsewhere then washed. Surviving clones were stained by crystal violet 14 days later. Only clones representing more than 50 cells were counted. Quantitative data (mean percentages \pm s.d., triplicates) are provided on each image. Three asterisks indicate statistically significant ($P < 0.001$) effects of the combination as compared to other treatments. Two asterisks indicate $P < 0.01$. Each experiment has been repeated two to four times, yielding similar results. A full colour version of this figure is available at the *Oncogene* journal online.

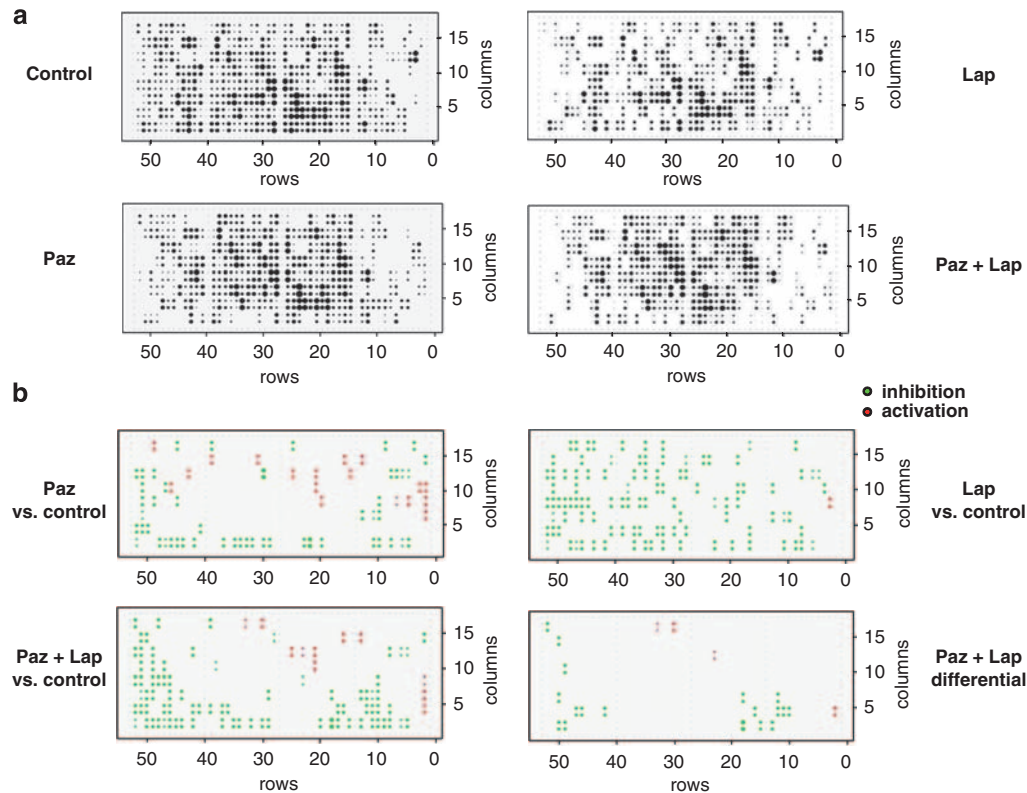


Figure 4 Kinome analyses. (a) Normalized representation of the four tyrosine kinase peptide microarray slides, each treated with the indicated A549 cell lysate. Cells were treated with 20 μ M of pazopanib (Paz) or 10 μ M of lapatinib (Lap) for 12 h or both. Then, cytoplasmic extracts were generated and tested for their capacity to phosphorylate an array of peptides immobilized on a glass slide. Each black spot corresponds to a known peptide sequence that has been phosphorylated by kinases present in the lysate. Nonphosphorylated sequences appear as negative (no visible spot). (b) Virtual representation of differential spot intensities. Green spots indicate an inhibition (inhibited kinases) and red spots activation (activated kinases) of the experimental values with respect to their controls. The lower right diagram represents the specific differential activation/inhibition of kinases by the combination regimen as compared to single treatments (Table 1). The complete list of modified tyrosine kinases is given in Supplementary Table S1. This experiment has been repeated twice, yielding comparable results. A full colour version of this figure is available at the *Oncogene* journal online.

tyrosine kinase activities (such as c-Met kinase) down to background levels, although each of the inhibitors alone had marginal or partial effects on their activity (Figure 4b; Table 1). These results indicate that pazopanib and lapatinib can provoke the ‘collapse’ of selected portions of the kinome, if they act concomitantly. In this context, it is particularly interesting that the combination of lapatinib and pazopanib led to a complete inhibition of c-Met. Indeed, it has been reported that c-Met inhibition—together with EGFR inhibition—has a synergistic antiproliferative effect on non-small-cell lung cancer cell lines *in vitro*, including the A549 cells that were used in our experiments (Puri and Salgia, 2008). Moreover c-Met inhibition alone suppresses the proliferation of A549 cells that were xenografted on immunodeficient mice (Puri *et al.*, 2007), underscoring that the inhibition of c-Met likewise contributes to the synergistic activity of lapatinib and pazopanib. Whether additional kinases that co-inhibited by lapatinib and pazopanib may contribute to their synergistic cytotoxicity remains elusive. However, it appears that the combined inhibition of lapatinib- and pazopanib-sensitive kinases can lead to the pronounced

inhibition of several kinases with known pro-survival activities (see Concluding remarks).

To further evaluate the functional impact of pazopanib and lapatinib on non-small-cell lung cancer cells, we evaluated the consequences of pazopanib and lapatinib on the transcriptome. The expression analyses were again performed at 12 h, using concentrations of lapatinib and pazopanib that cause 50% of the cells to enter an early phase of apoptosis at 24 h (defined by the collapse of the mitochondrial transmembrane potential) (Castedo *et al.*, 2002). This design was chosen based on the fact that at 12 h less than 10% of the cells had entered early apoptosis in response to the combination of both agents. We reasoned that it would be important to define transcriptome changes that occur during the proapoptotic signaling phase rather than those occurring during the execution of the apoptotic program (Castedo *et al.*, 2006; Vitale *et al.*, 2007; de La Motte Rouge *et al.*, 2007), when RNAs (Houge *et al.*, 1995; Nadano and Sato, 2000) and the death-associated bioenergetic collapse (Thompson *et al.*, 2004; Klawitter *et al.*, 2009) may affect the transcriptome in a nonspecific manner. Microarray analyses revealed that

Table 1 List of kinases from lower right panel in Figure 4b (i.e. those that are specifically modified in the combined treatment), as well as their fold-change values for each experimental condition

Kinase	Sequence	Substrate	Signal intensity compared to control (%)			P-value
			Paz	Lap	Paz + Lap	
Fyn	N-A-S-L-E-S-L-Y-S-A-C-S-M-Q-S	Growth factor receptor-bound protein 10	100	100	> 1000	0.0117
Src	C-K-N-V-V-P-L-Y-D-L-L-L-E-M-L	Estrogen receptor- α	100	100	> 1000	0.0096
Fyn	T-P-E-L-L-E-R-Y-N-M-E-R-D-I-N	PLC γ 2	100	100	> 1000	0.0076
Met	X-X-X-ED-ED-X-Y-V-P-X-X-X-X	Consensus sequence	100	100	0	0.0021
FGFR1	K-G-A-M-A-A-T-Y-S-A-L-N-R-N-Q	S6K- α 3	100	35	0	0.0016
ZAP70	S-G-E-D-D-D-Y-E-S-P-N-E-E-E	Consensus sequence	100	35	0	0.0018
ALK	F-S-L-A-A-I-N-Y-R-F-K-G-E-E-K	Consensus sequence	100	15	0	0.0014
Abl	S-R-I-G-D-E-L-Y-L-E-P-L-E-D-G	Rad9	100	5	0	0.0017
TGF β R2	G-Q-V-G-T-A-R-Y-M-A-P-E-V-L-E	TGF β R2	50	200	0	0.0014
TRKB	E-G-R-A-E-P-D-Y-G-A-L-Y-E-G-R	Consensus sequence	35	100	0	0.001
Fgr	R-L-I-K-D-D-E-Y-N-P-C-Q-G-S-K	Fgr	35	50	0	0.0016
FGFR3	R-R-P-P-G-L-D-Y-S-F-D-T-C-K-P	FGFR-3	15	50	0	0.0015
FGFR1	S-K-A-Q-Q-G-L-Y-Q-V-P-G-P-S-P	PI30Cas	50	35	0	0.0016
ZAP70	R-D-A-M-V-R-D-Y-V-R-Q-T-W-K-L	ZAP70	10	35	0	0.0009
EGFR	R-L-D-G-E-N-I-Y-I-R-H-S-N-L-M	Protein 4.1	20	25	0	0.002
FLT1	G-S-S-D-D-V-R-Y-V-N-A-F-K-F-M	VEGFR-1	15	25	0	0.0014
FAK	K-D-N-F-D-S-F-Y-S-E-V-A-E-L-G	Triple functional domain protein	25	15	0	0.0014

Given as percentage of signal intensity compared to untreated control cells.

pazopanib and lapatinib, given together, influenced the expression of a selected set of genes that were not affected by either of the tyrosine kinase inhibitors alone (Figure 5a). A total of 174 RNA species that were overexpressed or downregulated after the combination treatment were not influenced in the same manner by either pazopanib or lapatinib alone (Figure 5b; Table 2; Supplementay Table S2). These analyses hence suggest that selective combination effects of pazopanib and lapatinib may predict their synergistic toxicity on non-small-cell lung cancer cells.

Synergistic anticancer activity of pazopanib and lapatinib on multiple carcinoma cell lines

On the basis of aforementioned results, we suspected that the transcriptome effects of pazopanib and lapatinib might indicate synergistic cytotoxic activities of both tyrosine kinase inhibitors. We therefore validated the set of 174 mRNAs (Figure 5b) whose expression level is up- or downregulated by pazopanib and lapatinib in A549 cells on a panel of distinct carcinoma cells representing non-small-cell lung cancer (H1975 carrying an EGFR mutation abolishing erlotinib-mediated antiproliferative effects and H1299 with mutated p53), gastric cancer (AGS) and colon cancer (HCT116). A significant fraction of the mRNA species (33%) identified in the initial A549 screen were modulated in the same manner by the combination of pazopanib and lapatinib (but not by other chemotherapeutic agents such as cisplatin, or drug combinations; data not shown) in all the cell lines (Figure 5c; Supplementary Table S3), suggesting that pazopanib and lapatinib might exert synergistic effects on multiple different malignancies. Among the 58 genes that were induced specifically by the combination regimen in all cell lines, several have previously been involved in

apoptotic signaling, in particular *p53* (Pietsch *et al.*, 2008), *PHLDA1* (also known as T-cell-death-associated gene 51, *TDAG51*) (Hayashida *et al.*, 2006; Joo *et al.*, 2007; Oberst *et al.*, 2008) and *RHOT1* (ras homolog gene family, member T1; also known as mitochondrial Rho; *Miro1*) (Fransson *et al.*, 2003). Indeed, we observed that the combination of pazopanib and lapatinib was able to kill the five carcinoma cell lines included in the transcriptome analysis, as well as ovarian (SKOV3) and cervix cancer cells (HeLa), yielding highly significant synergistic effects of both compounds as compared to each of them alone (Figure 5d; Supplementary Table S4). In conclusion, pazopanib and lapatinib may cooperate to mediate generally cytotoxic effect on multiple carcinomas.

Concluding remarks

We report here the unexpected finding that the use of tyrosine kinase inhibitors designed to inhibit HER1/HER2 and VEGFR can exert synergistic cytotoxic effects on a variety of carcinoma cell lines. Synergistic anticancer effects are potentially interesting for the clinical application of drugs, following the dual aim of reducing side effects (by reducing the concentration of the agents used for anticancer therapy) and improving therapeutic efficacy (by obtaining systemic lethal effects on tumor cells). It has been shown in the past that inhibition of HER1 can induce cell death in HER1-dependent cancer cells (Helfrich *et al.*, 2006), and it has also been shown that inhibition of VEGFR can exert direct (cell-autonomous) effects on VEGFR-expressing tumor cells, beyond the angiostatic (non-cell-autonomous) effects of VEGFR inhibitors on endothelial cells (Fan *et al.*, 2005; Bianco *et al.*, 2008; Simiantonaki *et al.*, 2008; Sini *et al.*, 2008). Here, we show that pazopanib and lapatinib together are much more potent in their

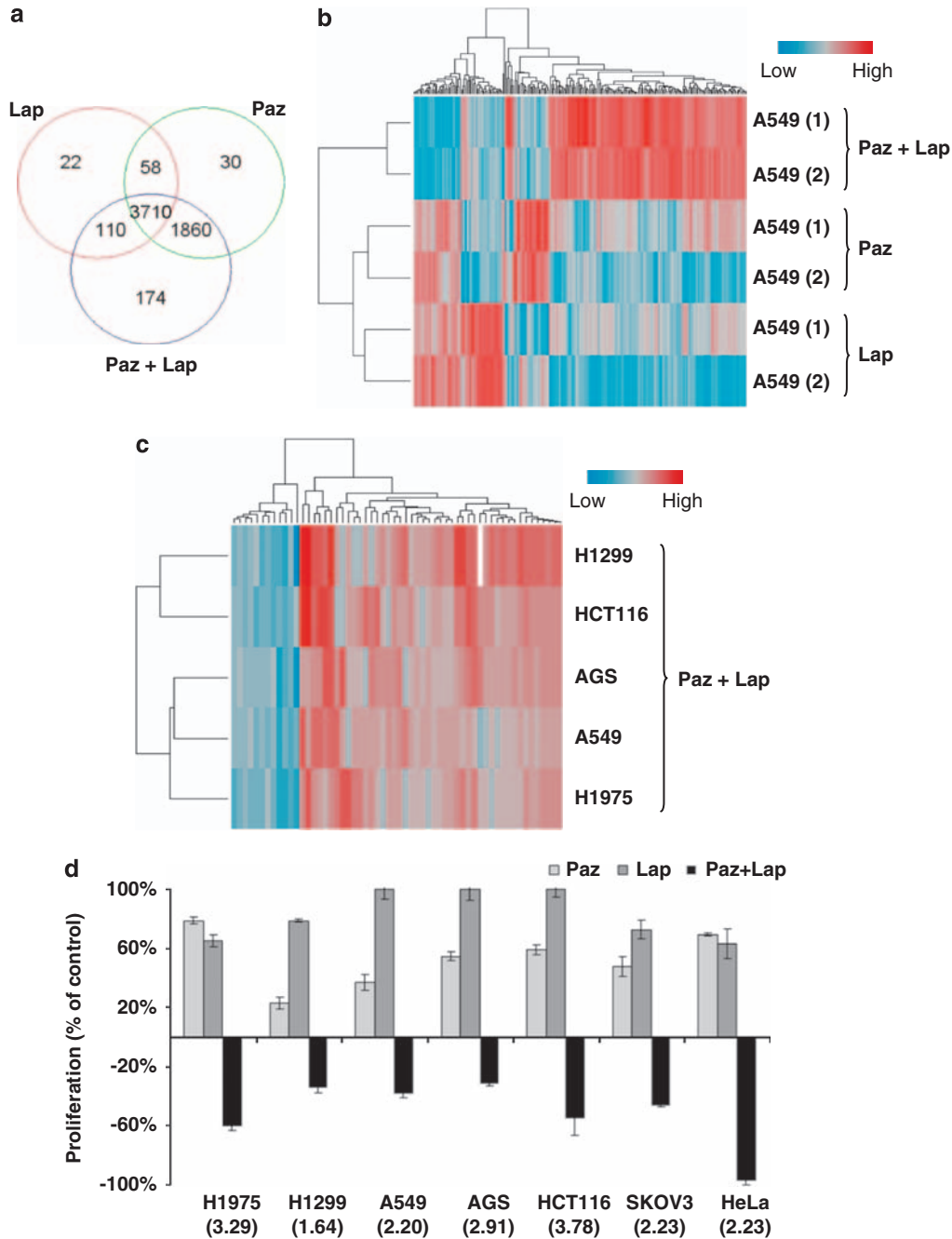


Figure 5 Gene expression of A549 cells and effect of pazopanib and lapatinib in other cell lines. mRNA was extracted from cells that had been treated with 20 μM of pazopanib (Paz) or 10 μM of lapatinib (Lap) for 12 h or both. At this time point, the combination of both agents induced less than 10% of apoptosis. **(a)** Venn diagram representation of the number of genes in A549 cells that are common or specific to each treatment condition. Genes (174) are specifically modified in the pazopanib/lapatinib drug combination. **(b)** Two-dimensional hierarchical clustering of the 174 genes in A549 cells whose expression is modified in a statistically significant manner (FDR < 0.05) in drug-combination treatment compared with each single drug treatment. Each row represents the combination of two dye-swap experimental samples, and each column a single gene. Table 2 is associated with **b** and reports selected examples of the differential transcriptional effects promoted by the combined treatment of pazopanib/lapatinib compared to single treatments and controls. Supplementary Table S2 contains the complete list of the 174 gene modulations. **(c)** Gene expression analysis of cell lines from related (lung) and unrelated carcinomas (gastric and colon). Of the 174 genes in the A549-signature, 58 were found as significantly modified in all cell lines treated with the pazopanib/lapatinib combination (q -value < 0.05). The complete list of these 58 Paz/Lap-specific genes with fold changes in each cell line is given in Supplementary Table S3. These genes were not modified similarly in other proapoptotic conditions (data not shown). **(d)** Effects on proliferation in different cell lines. By considering the T_0 absorbance and comparing values to nontreated controls, the combination clearly shows a cytotoxic effect on all studied cell lines (negative values). The Bliss index for synergy is given in brackets under each cell line and was calculated as the ratio Observed/Expected, so an index = 1 indicates additive effects, whereas index < 0 and > 1 indicate, respectively, antagonistic and synergistic effects. The details of Bliss index calculation are given in Supplementary Table S4.

Table 2 Selected examples (see complete list in Supplementary Table S2) of the differential transcriptional effects in A549 cells promoted by single or combined treatments of pazopanib and lapatinib

Gene name	EntrezGen ID	Gene family	Expression compared to control (%)		
			Paz	Lap	Paz + Lap
EPPK1	83481	other	150	85	701
CDH4	1002	other	136	67	566
RHOT1	55288	enzyme	101	124	372
MON2	23041	other	109	96	345
SLC16A6	9120	transporter	116	91	318
EGFR	1956	kinase	108	84	312
ZNF507	22847	other	83	121	280
PRDM1	639	transcription regulator	120	83	271
ZNF19	7567	transcription regulator	105	84	261
ZC3H13	23091	other	131	82	249
VPS13B	157680	transporter	91	92	247
CLDN12	9069	other	97	158	216
TP53	7157	transcription regulator	120	113	212
PHLDA1	22822	other	110	96	192
MET	4233	kinase	119	152	188
VCP1P1	80124	peptidase	90	100	49
CDADC1	81602	kinase	104	104	47
LOC149134	149134	other	98	101	44
IFNAR2	3455	transmembrane receptor	79	108	42
EGR1	1958	transcription regulator	112	87	41

The values are given in percent gene expression as compared to expression in untreated control cells.

antiproliferative and proapoptotic activities than either of the two agents alone. In support of these findings, a recent article reported a supraadditive effect of a dual HER1/VEGFR inhibition (gefitinib + AZD2171) in head and neck cancer xenografts (Bozec *et al.*, 2007) and preliminary data in patients with breast cancer suggested clinical activity of pazopanib and lapatinib when administered as a combination (Sloan and Scheinfeld, 2008). However, it would be premature to conclude that the specific inhibition of HER1, HER2 and VEGFR has a synergistic effect. Indeed, both pazopanib and lapatinib are not uniquely specific inhibitors of HER1/HER2 and VEGFR, respectively, and rather inhibit multiple tyrosine kinases (Karaman *et al.*, 2008). Although we did not assess the complete repertoire of tyrosine kinases targeted directly by these agents, the characterization of the kinome influenced by pazopanib and lapatinib suggests that both agents can inhibit (directly or indirectly) 50–100 different tyrosine kinase activities independently, at least at the relatively high concentrations used here. Indeed, emerging clinical data are suggesting the benefit of high-dose pulse treatments of tyrosine kinase inhibitors in combination with other molecules in cancer patients (Chien *et al.*, 2008; Riely *et al.*, 2009). Thus, at concentrations that should be therapeutically relevant, both pazopanib and lapatinib can influence multiple kinases, well beyond the narrow range of activities that has been defined for them (VEGFR-1, -2, -3; PDGFR and c-kit for pazopanib, and HER1 and HER2 for lapatinib). Of note, the combination of pazopanib and lapatinib suppressed the activity of some kinases by 100% although each kinase inhibitor on its own exerted only partial effects. This is true, in particular, for c-Met, a kinase whose activity

was completely extinguished by pazopanib and lapatinib. Inhibition of c-Met has been shown to exert cytotoxic effects on A549 cells (Puri *et al.*, 2007), suggesting that c-Met inhibition might explain some of the synergy of the pazopanib/lapatinib combination. How this ‘combined’ blockade of c-Met is achieved remains unknown. However, it is possible that the inhibition of other kinases may indirectly affect c-Met (Peruzzi and Bottaro, 2006; Comoglio *et al.*, 2008). However, beyond c-Met, the complete inhibition of FGFR, ZAP70, ALK and FAK activation that we observed in the condition of combined treatment can also have proapoptotic effects (Golubovskaya *et al.*, 2002; Danilov *et al.*, 2005; Mourali *et al.*, 2006; Calandrella *et al.*, 2007). Of note, lapatinib has previously shown a dose- and time-dependent effect on phosphoproteins such as FOXO3A and its target protein p27 (Hegde *et al.*, 2007). It is not known how such time-dependent effects would affect our observations.

Before any signs of apoptosis were detectable, pazopanib and lapatinib induced a major change in the transcriptome leading to the specific induction of a panel of proapoptotic mRNA species that was first retrieved among A549 cells and then validated on a series of additional non-small-cell lung cancers and a diverse array of unrelated carcinoma cell lines. Although the exact molecular mechanisms that link the extinction of tyrosine kinase activities to changes in gene expression remain elusive, these results point to the possibility to identify biomarkers that predict a therapeutic response induced by pazopanib together with lapatinib, as well as giving new insight as to better understand the hyperadditive action of both tyrosine kinase inhibitors. Anyhow, our data support further implementation of clinical trials associating lapatinib

and pazopanib at various schedules and dosages in different cancers.

Materials and methods

Cell lines and culture

All cell lines were purchased from the ATCC cell collection. A549 and AGS cells were grown in F12-K medium from Gibco-Invitrogen (Carlsbad, CA, USA) containing L-glutamine, supplemented with 10% fetal calf serum (FCS), 100 U/ml penicillin G sodium and 100 µg/ml streptomycin sulfate. H1299 and H1975 cells were maintained in RPMI 1640 medium with GlutaMAX supplemented with 10% FCS and antibiotics (as above). HCT116 and SKOV3 cells were grown in McCoy's 5A medium supplemented with 10% FCS. HeLa cells were grown in Dulbecco's modified Eagle's medium (DMEM) supplemented with 10% FCS, 100 U/ml penicillin, 100 mg/ml streptomycin and hygromycin B (125 mg/ml) under 5% CO₂. For proliferation assays, all cell lines were cultured in DMEM/F12 (1:1) with L-glutamine but no phenol red supplemented with 10% FCS and 100 U/ml penicillin, 100 mg/ml streptomycin.

Drug preparations

Pazopanib (GW786034B) and lapatinib (GW572016F) were obtained from GlaxoSmithKline (Brentford, UK) and dissolved in neat dimethyl sulfoxide (DMSO) at 10 mM and conserved in small aliquots at -20 °C. All experiments were designed to obtain an equal amount of DMSO in every well. Cisplatin (CDDP) was dissolved in DMSO at 100 mM, and pemetrexed (Alimta, Eli Lilly, Indianapolis, IN, USA) was diluted at 10 mM in water and conserved as aliquots at -20 °C.

Cell proliferation assay

For proliferation assays, 25 × 10³ cells per ml were seeded in triplicates in 96-well plates (2500 cells per well) 18 h before the treatment with pazopanib, lapatinib, cisplatin and/or pemetrexed at concentrations varying from 5 to 40 µM. Treatments were prolonged for 48 or 72 h before the assessment of end-point cell proliferation. As recommended by Monks *et al.* (1991), cell proliferation was quantified at time zero (T₀, the time at which the drugs were added) and at end point (T₄₈ or T₇₂, 48 and 72 h after T₀) by means of a colorimetric assay, which measures the conversion of the colorless tetrazolium salt WST-1 (4-[3-(4-iodophenyl)-2-(4-nitrophenyl)-2H-5-tetrazolo]-1,3-benzene disulfonate) to formazan (λ = 450 nm) catalysed by cellular dehydrogenases. For this, the Cell Proliferation Reagent WST-1 (Roche Applied Science, Penzberg, Germany) was used.

Assessment of apoptosis and cell-cycle distribution

A549 cells were incubated in triplicate wells for 72 h with 8 µM of pazopanib, or 10 µM of lapatinib or both. These concentrations were chosen for their cytotoxic effect on A549 cells in the proliferation assays (loss of cells compared to T₀). Apoptotic cells were quantified by cytofluorometric analysis using a FACSVantage apparatus (Becton Dickinson, Mountain View, CA, USA) as described previously (Zamzami and Kroemer, 2004). Thus, after trypsination, cells were washed and then stained with propidium iodide (PI; 1 µg/ml; Sigma, Steinheim, Germany) and with either DiOC₆(3) (3,3-dihexyloxacarbocyanine iodide; 40 nM; Molecular Probes, Eugene, OR, USA) for 15 min at 37 °C to determine the mitochondrial transmembrane potential, or the Annexin V antibody (BD Pharmingen, San Diego, CA, USA) as recommended by the manufacturer.

For cell-cycle analyses, cells were harvested, washed and stained with Hoechst 33342 (10 µg/ml; Invitrogen) followed by an incubation period of 30 min at room temperature. Subsequently cell-cycle distribution was determined by cytofluorometric analysis.

Microscopic evaluation of dying cells

For microscopic evaluation, A549 cells were seeded on LabTek slides (Nalge Nunc, Naperville, IL, USA), previously treated with polylysine. After 72 h of drug treatment (8 µM of pazopanib, 10 µM of lapatinib or both) the LabTek slides were centrifuged and cells stained with Hoechst 33342 (10 µg/ml) and PI (1 µg/ml). Slides were mounted and cells were evaluated under a Leica Microsystems (Wetzlar, Germany) confocal microscope.

Clonogenic assay

A549 cells were incubated in triplicate for 72 h with 8 µM of pazopanib, or 10 µM of lapatinib or both, and washed with growth medium before long-term incubation. Clones were stained in crystal violet according to standard procedures after 14 days of incubation. Only clones representing more than 50 cells were counted.

Extraction of RNA and whole-cell lysate preparations

Cells were seeded at 50 000 cells per ml in six-well plates (2 ml per well) in duplicate. Each cell line was treated after 18 h of cell culture stabilization. For kinome and transcription analysis, the treatment duration was 12 h (before the appearance of apoptotic effects) using drug concentrations that demonstrated cytotoxic effect on all cell lines (20 µM pazopanib and 10 µM lapatinib). In controls, drugs were replaced with medium containing DMSO at equivalent concentrations. For kinase assays, whole-cell lysates were prepared according to standard established protocols. Briefly, the cells were washed three times in cold phosphate-buffered saline, solubilized with cell lysis buffer (Cell Signaling Technology, Boston, MA, USA) and gently homogenized. After 30 min on ice, cellular fragments were precipitated at 10 000 r.p.m. in a cold centrifuge and the quantification of the protein concentration was determined by the DC protein assay (Bio-Rad, Hercules, CA, USA). For transcriptome analysis, cultures were stopped at T₁₂ by addition of 400 µl of RLT buffer (Qiagen, Hilden, Germany). RNAs were extracted using RNeasy Micro Kit (Qiagen) according to the manufacturer's recommendations. Briefly, 350 µl of lysate was collected from each well. RNAs were precipitated with equal volume of ethanol 80% and placed into spin columns. After centrifugation RNAs were washed with RW1 reagent and treated with DNase for 15 min at room temperature. After washes, RNAs were eluted with 14 µl of RNase-free distilled water, quantified and qualified with Nanodrop ND-1000 spectrometer and Bioanalyser-2100 (Agilent, Santa Clara, CA, USA).

Kinome analysis

After determination of protein concentrations in cell lysates, these (200 µg per array) were applied on CelluSpot Tyrosine-kinase substrates I microarrays (Intavis Bioanalytical Instruments, Koeln, Germany) in tyrosine kinase buffer (Cell Signaling Technology) with 1% bovine serum albumin for 1 h and 30 min at room temperature. The microarray slides were then incubated with antibodies specific for tyrosine phosphopeptides (horseradish-peroxidase-conjugated mouse monoclonal anti-phosphotyrosine antibody (R&D Systems,

Minneapolis, MN, USA) before revelation by means of ECL Detection kit (Amersham Pharmacia, Pittsburgh, PA, USA) and Hyperfilm X-ray films (Amersham Pharmacia). Quantification of spots was performed using a camera in the Syngene GBox (Ozyme, Saint Quentin en Yvelines, France) and its associated image software.

Gene expression analysis

Gene expression analysis was performed by dual-color competitive hybridization on Agilent 4 × 44K gene expression microarrays, according to the manufacturer's recommendations. Briefly, 500 ng of RNA, extracted as previously described, was transcribed into cDNA. cRNA probes were synthesized with T7 RNA polymerase and labeled by incorporation of CTP-cyanine 3 for untreated control cells and CTP-cyanine 5 for treated cells. Each treated cell line was hybridized against its corresponding untreated control overnight at 65 °C. After washes, slides were digitized into the Agilent scanner station. Quality controls and ratio calculation were performed with Feature Extraction software (Agilent), and data were transferred into R software for statistical analysis.

Calculations and statistical analysis

The analysis of the effect of drug treatments on cell survival was performed by calculating an inhibition index (called 'Effect') from the absorbance measurements (optical density, OD), after blank deduction, as follows (Monks *et al.*, 1991):

$$\text{Effect} = \begin{cases} \left[1 - \frac{\text{Treated} - T_0}{\text{Control} - T_0} \right] \times 100 & \text{if Treated} \geq T_0 \\ \left[1 - \frac{\text{Treated} - T_0}{T_0} \right] \times 100 & \text{if else} \end{cases}$$

This transformation has the advantage of giving values from 0 to 200 that are increasing directly in relation to the effect due to each treatment condition. If the score equals 0, the effect is null (control condition). If the score is 100, the number of cell is equivalent to T_0 ($\text{OD.treated} = \text{OD} \times T_0$), meaning there is a complete cytostatic effect. Finally, if the score is between 100 and 200, the effect is cytotoxic.

Computational analysis. Research of significant growth inhibition effects was performed with R software (version 2.6.1,

References

- Barnes CJ, Kumar R. (2003). Epidermal growth factor receptor family tyrosine kinases as signal integrators and therapeutic targets. *Cancer Metastasis Rev* **22**: 301–307.
- Bianco R, Rosa R, Damiano V, Daniele G, Gelardi T, Garofalo S *et al.* (2008). Vascular endothelial growth factor receptor-1 contributes to resistance to anti-epidermal growth factor receptor drugs in human cancer cells. *Clin Cancer Res* **14**: 5069–5080.
- Bliss CI. (1939). The toxicity of poisons applied jointly. *Ann Appl Biol* **26**: 585–615.
- Bozec A, Formento P, Lassalle S, Lippens C, Hofman P, Milano G. (2007). Dual inhibition of EGFR and VEGFR pathways in combination with irradiation: antitumour supra-additive effects on human head and neck cancer xenografts. *Br J Cancer* **97**: 65–72.
- Calandrella N, Risuleo G, Scarsella G, Mustazza C, Castelli M, Galati F *et al.* (2007). Reduction of cell proliferation induced by PD166866: an inhibitor of the basic fibroblast growth factor. *J Exp Clin Cancer Res* **26**: 405–409.
- Cameron DA, Stein S. (2008). Drug Insight: intracellular inhibitors of HER2—clinical development of lapatinib in breast cancer. *Nat Clin Pract Oncol* **5**: 512–520.
- Castedo M, Coquelle A, Vivet S, Vitale I, Kauffmann A, Dessen P *et al.* (2006). Apoptosis regulation in tetraploid cancer cells. *EMBO J* **25**: 2584–2595.
- Castedo M, Ferri K, Roumier T, Metivier D, Zamzami N, Kroemer G. (2002). Quantitation of mitochondrial alterations associated with apoptosis. *J Immunol Methods* **265**: 39–47.
- Chien AJ, Illi JA, Ko AH, Dubey S, Jahan TM, Hylton NM *et al.* (2008). A phase I dose escalation study of a 2 day lapatinib chemosensitization pulse preceding weekly intravenous nanoparticle albumin-bound paclitaxel (nab-paclitaxel) in patients with advanced cancer. *J Clin Oncol* **26**: Abstract number 3595.
- Ciardello F, Tortora G. (2008). EGFR antagonists in cancer treatment. *N Engl J Med* **358**: 1160–1174.
- Comoglio PM, Giordano S, Trusolino L. (2008). Drug development of MET inhibitors: targeting oncogene addiction and expedience. *Nat Rev Drug Discov* **7**: 504–516.

2007-11-26) by using a response surface method where the full model was initially supposed to be of the form:

$$Y = \text{Log} \left(\frac{\text{Effect}}{\text{Effect}_{\text{Max}} - \text{Effect}} \right) \\ = \alpha + \beta \cdot \text{Paz} + \gamma \cdot \text{Lap} + \delta \cdot \text{Paz} \cdot \text{Lap}$$

where $(\alpha, \beta, \gamma, \delta)' = (X'X)^{-1}X'Y$

To compare drug effects between different cell lines, we calculated the index of Bliss (Bliss, 1939). First, an inhibition score was calculated as above, taking values between 0 and 200. The expected effect of the combination was then estimated from each separate drug effect: $E_{\text{Exp}} = E_{\text{Paz}} + E_{\text{Lap}} - (E_{\text{Paz}} \cdot E_{\text{Lap}})$ and a ratio Observed/Expected was calculated. An index = 1 indicates an additive effect, whereas index < 0 and > 1 indicate, respectively, antagonistic and synergistic effect of the combination.

To identify a specific gene expression signature associated with the pazopanib/lapatinib combination on A549 cell lines, we used a *limma* procedure (Wettenhall and Smyth, 2004). An initial filtering was applied to include only sequences that were significantly modified ($P < 10^{-3}$) in each treatment condition (in both duplicates). The A549 pazopanib/lapatinib signature was then studied on other cell lines by using a *sam* procedure (Wu, 2006). The *q*-value calculation was used as false discovery rate procedure control, according to Storey and Tibshirani (2003).

Conflict of interest

The authors declare no conflict of interest.

Acknowledgements

GK received grants from Ligue Nationale contre le Cancer (équipe labellisée), Agence Nationale de Recherche, Institut National contre le Cancer, Cancéropôle Ile-de-France, European Union (Active p53, ApoSys, ChemoRes, DeathTrain, RIGHT, TransDeath) and Fondation pour la Recherche Médicale.

- Danilov AV, Klein AK, Lee HJ, Baez DV, Huber BT. (2005). Differential control of G0 programme in chronic lymphocytic leukaemia: a novel prognostic factor. *Br J Haematol* **128**: 472–481.
- de La Motte Rouge T, Galluzzi L, Olaussen KA, Zermati Y, Tasmemir E, Robert T *et al.* (2007). A novel epidermal growth factor receptor inhibitor promotes apoptosis in non-small cell lung cancer cells resistant to erlotinib. *Cancer Res* **67**: 6253–6262.
- Donnem T, Al-Saad S, Al-Shibli K, Delghandi MP, Persson M, Nilsen MN *et al.* (2007). Inverse prognostic impact of angiogenic marker expression in tumor cells versus stromal cells in non small cell lung cancer. *Clin Cancer Res* **13**: 6649–6657.
- Druker BJ, Talpaz M, Resta DJ, Peng B, Buchdunger E, Ford JM *et al.* (2001). Efficacy and safety of a specific inhibitor of the BCR-ABL tyrosine kinase in chronic myeloid leukemia. *N Engl J Med* **344**: 1031–1037.
- Edinger AL. (2007). Controlling cell growth and survival through regulated nutrient transporter expression. *Biochem J* **406**: 1–12.
- Fan F, Wey JS, McCarty MF, Belcheva A, Liu W, Bauer TW *et al.* (2005). Expression and function of vascular endothelial growth factor receptor-1 on human colorectal cancer cells. *Oncogene* **24**: 2647–2653.
- Flier JS, Mueckler MM, Usher P, Lodish HF. (1987). Elevated levels of glucose transport and transporter messenger RNA are induced by ras or src oncogenes. *Science* **235**: 1492–1495.
- Fransson A, Ruusala A, Aspenstrom P. (2003). Atypical Rho GTPases have roles in mitochondrial homeostasis and apoptosis. *J Biol Chem* **278**: 6495–6502.
- Geyer CE, Forster J, Lindquist D, Chan S, Romieu CG, Pienkowski T *et al.* (2006). Lapatinib plus capecitabine for HER2-positive advanced breast cancer. *N Engl J Med* **355**: 2733–2743.
- Golubovskaya V, Beviglia L, Xu LH, Earp 3rd HS, Craven R, Cance W. (2002). Dual inhibition of focal adhesion kinase and epidermal growth factor receptor pathways cooperatively induces death receptor-mediated apoptosis in human breast cancer cells. *J Biol Chem* **277**: 38978–38987.
- Harris PA, Bolor A, Cheung M, Kumar R, Crosby RM, Davis-Ward RG *et al.* (2008). Discovery of 5-[[4-[(2,3-dimethyl-2H-indazol-6-yl)methylamino]-2-pyrimidinyl]amino]-2-methyl-benzenesulfonamide (Pazopanib), a novel and potent vascular endothelial growth factor receptor inhibitor. *J Med Chem* **51**: 4632–4640.
- Hayashida N, Inouye S, Fujimoto M, Tanaka Y, Izu H, Takaki E *et al.* (2006). A novel HSF1-mediated death pathway that is suppressed by heat shock proteins. *EMBO J* **25**: 4773–4783.
- Hegde PS, Rusnak D, Bertiaux M, Alligood K, Strum J, Gagnon R *et al.* (2007). Delineation of molecular mechanisms of sensitivity to lapatinib in breast cancer cell lines using global gene expression profiles. *Mol Cancer Ther* **6**: 1629–1640.
- Helfrich BA, Raben D, Varella-Garcia M, Gustafson D, Chan DC, Bemis L *et al.* (2006). Antitumor activity of the epidermal growth factor receptor (EGFR) tyrosine kinase inhibitor gefitinib (ZD1839, Iressa) in non-small cell lung cancer cell lines correlates with gene copy number and EGFR mutations but not EGFR protein levels. *Clin Cancer Res* **12**: 7117–7125.
- Houge G, Robaye B, Eikhom TS, Golstein J, Mellgren G, Gjertsen BT *et al.* (1995). Fine mapping of 28S rRNA sites specifically cleaved in cells undergoing apoptosis. *Mol Cell Biol* **15**: 2051–2062.
- Hult J, Lee RJ, Russell RG, Pestell RG. (2002). ErbB-2-induced mammary tumor growth: the role of cyclin D1 and p27Kip1. *Biochem Pharmacol* **64**: 827–836.
- Hurwitz HI, Dowlati A, Saini S, Savage S, Suttle AB, Gibson DM *et al.* (2009). Phase I trial of pazopanib in patients with advanced cancer. *Clin Cancer Res* **15**: 4220–4227.
- Johnson SA, Hunter T. (2005). Kinomics: methods for deciphering the kinome. *Nat Methods* **2**: 17–25.
- Joo JH, Liao G, Collins JB, Grissom SF, Jetten AM. (2007). Farnesol-induced apoptosis in human lung carcinoma cells is coupled to the endoplasmic reticulum stress response. *Cancer Res* **67**: 7929–7936.
- Karaman MW, Herrgard S, Treiber DK, Gallant P, Atteridge CE, Campbell BT *et al.* (2008). A quantitative analysis of kinase inhibitor selectivity. *Nat Biotechnol* **26**: 127–132.
- Kerbel RS. (2008). Tumor angiogenesis. *N Engl J Med* **358**: 2039–2049.
- Klawitter J, Zhang YL, Anderson N, Serkova NJ, Christians U. (2009). Development and validation of a sensitive assay for the quantification of imatinib using LC/LC-MS/MS in human whole blood and cell culture. *Biomed Chromatogr* (e-pub ahead of print 10 June 2009).
- Konecny GE, Pegram MD, Venkatesan N, Finn R, Yang G, Rahmeh M *et al.* (2006). Activity of the dual kinase inhibitor lapatinib (GW572016) against HER-2-overexpressing and trastuzumab-treated breast cancer cells. *Cancer Res* **66**: 1630–1639.
- Kroemer G, Galluzzi L, Vandenabeele P, Abrams J, Alnemri ES, Baehrecke EH *et al.* (2009). Classification of cell death: recommendations of the Nomenclature Committee on Cell Death 2009. *Cell Death Differ* **16**: 3–11.
- Kumar R, Knick VB, Rudolph SK, Johnson JH, Crosby RM, Crouthamel MC *et al.* (2007). Pharmacokinetic-pharmacodynamic correlation from mouse to human with pazopanib, a multikinase angiogenesis inhibitor with potent antitumor and antiangiogenic activity. *Mol Cancer Ther* **6**: 2012–2021.
- Lee TH, Seng S, Sekine M, Hinton C, Fu Y, Avraham HK *et al.* (2007). Vascular endothelial growth factor mediates intracrine survival in human breast carcinoma cells through internally expressed VEGFR1/FLT1. *PLoS Med* **4**: e186.
- Manning G, Whyte DB, Martinez R, Hunter T, Sudarsanam S. (2002). The protein kinase complement of the human genome. *Science* **298**: 1912–1934.
- Monks A, Scudiero D, Skehan P, Shoemaker R, Paull K, Vistica D *et al.* (1991). Feasibility of a high-flux anticancer drug screen using a diverse panel of cultured human tumor cell lines. *J Natl Cancer Inst* **83**: 757–766.
- Mourali J, Benard A, Lourenco FC, Monnet C, Greenland C, Moog-Lutz C *et al.* (2006). Anaplastic lymphoma kinase is a dependence receptor whose proapoptotic functions are activated by caspase cleavage. *Mol Cell Biol* **26**: 6209–6222.
- Nadano D, Sato TA. (2000). Caspase-3-dependent and -independent degradation of 28 S ribosomal RNA may be involved in the inhibition of protein synthesis during apoptosis initiated by death receptor engagement. *J Biol Chem* **275**: 13967–13973.
- Noble ME, Endicott JA, Johnson LN. (2004). Protein kinase inhibitors: insights into drug design from structure. *Science* **303**: 1800–1805.
- Oberst MD, Beberman SJ, Zhao L, Yin JJ, Ward Y, Kelly K. (2008). TDAG51 is an ERK signaling target that opposes ERK-mediated HME16C mammary epithelial cell transformation. *BMC Cancer* **8**: 189.
- Peruzzi B, Bottaro DP. (2006). Targeting the c-Met signaling pathway in cancer. *Clin Cancer Res* **12**: 3657–3660.
- Petit AM, Rak J, Hung MC, Rockwell P, Goldstein N, Fendly B *et al.* (1997). Neutralizing antibodies against epidermal growth factor and ErbB-2/neu receptor tyrosine kinases down-regulate vascular endothelial growth factor production by tumor cells *in vitro* and *in vivo*: angiogenic implications for signal transduction therapy of solid tumors. *Am J Pathol* **151**: 1523–1530.
- Pietsch EC, Sykes SM, McMahon SB, Murphy ME. (2008). The p53 family and programmed cell death. *Oncogene* **27**: 6507–6521.
- Podar K, Tonon G, Sattler M, Tai YT, Legouill S, Yasui H *et al.* (2006). The small-molecule VEGF receptor inhibitor pazopanib (GW786034B) targets both tumor and endothelial cells in multiple myeloma. *Proc Natl Acad Sci USA* **103**: 19478–19483.
- Press MF, Finn RS, Cameron D, Di Leo A, Geyer CE, Villalobos IE *et al.* (2008). HER-2 gene amplification, HER-2 and epidermal growth factor receptor mRNA and protein expression, and lapatinib efficacy in women with metastatic breast cancer. *Clin Cancer Res* **14**: 7861–7870.
- Puri N, Khramtsov A, Ahmed S, Nallasura V, Hetzel JT, Jagadeeswaran R *et al.* (2007). A selective small molecule inhibitor of c-Met,

- PHA665752, inhibits tumorigenicity and angiogenesis in mouse lung cancer xenografts. *Cancer Res* **67**: 3529–3534.
- Puri N, Salgia R. (2008). Synergism of EGFR and c-Met pathways, cross-talk and inhibition, in non-small cell lung cancer. *J Carcinog* **7**: 9.
- Riely GJ, Rizvi NA, Kris MG, Milton DT, Solit DB, Rosen N *et al.* (2009). Randomized phase II study of pulse erlotinib before or after carboplatin and paclitaxel in current or former smokers with advanced non-small-cell lung cancer. *J Clin Oncol* **27**: 264–270.
- Simiantonaki N, Jayasinghe C, Michel-Schmidt R, Peters K, Hermanns MI, Kirkpatrick CJ. (2008). Hypoxia-induced epithelial VEGF-C/VEGFR-3 upregulation in carcinoma cell lines. *Int J Oncol* **32**: 585–592.
- Sini P, Samarzija I, Baffert F, Littlewood-Evans A, Schnell C, Theuer A *et al.* (2008). Inhibition of multiple vascular endothelial growth factor receptors (VEGFR) blocks lymph node metastases but inhibition of VEGFR-2 is sufficient to sensitize tumor cells to platinum-based chemotherapeutics. *Cancer Res* **68**: 1581–1592.
- Sleijffer S, Wiemer E, Verweij J. (2008). Drug insight: gastrointestinal stromal tumors (GIST)—the solid tumor model for cancer-specific treatment. *Nat Clin Pract Oncol* **5**: 102–111.
- Sloan B, Scheinfeld NS. (2008). Pazopanib, a VEGF receptor tyrosine kinase inhibitor for cancer therapy. *Curr Opin Investig Drugs* **9**: 1324–1335.
- Sonpavde G, Hutson TE, Sternberg CN. (2008). Pazopanib, a potent orally administered small-molecule multitargeted tyrosine kinase inhibitor for renal cell carcinoma. *Expert Opin Investig Drugs* **17**: 253–261.
- Storey JD, Tibshirani R. (2003). Statistical methods for identifying differentially expressed genes in DNA microarrays. *Methods Mol Biol* **224**: 149–157.
- Storniolo AM, Pegram MD, Overmoyer B, Silverman P, Peacock NW, Jones SF *et al.* (2008). Phase I dose escalation and pharmacokinetic study of lapatinib in combination with trastuzumab in patients with advanced ErbB2-positive breast cancer. *J Clin Oncol* **26**: 3317–3323.
- Thompson HJ, Zhu Z, Jiang W. (2004). Identification of the apoptosis activation cascade induced in mammary carcinomas by energy restriction. *Cancer Res* **64**: 1541–1545.
- Vitale I, Galluzzi L, Vivet S, Nanty L, Dessen P, Senovilla L *et al.* (2007). Inhibition of Chk1 kills tetraploid tumor cells through a p53-dependent pathway. *PLoS ONE* **2**: e1337.
- Wettenhall JM, Smyth GK. (2004). limmaGUI: a graphical user interface for linear modeling of microarray data. *Bioinformatics* **20**: 3705–3706.
- Wood ER, Truesdale AT, McDonald OB, Yuan D, Hassell A, Dickerson SH *et al.* (2004). A unique structure for epidermal growth factor receptor bound to GW572016 (Lapatinib): relationships among protein conformation, inhibitor off-rate, and receptor activity in tumor cells. *Cancer Res* **64**: 6652–6659.
- Wu B. (2006). Differential gene expression detection and sample classification using penalized linear regression models. *Bioinformatics* **22**: 472–476.
- Zamzami N, Kroemer G. (2004). Methods to measure membrane potential and permeability transition in the mitochondria during apoptosis. *Methods Mol Biol* **282**: 103–115.

Supplementary Information accompanies the paper on the Oncogene website (<http://www.nature.com/onc>)